

Nonlinear Observer for Tightly Integrated Inertial Navigation Aided by Pseudo-Range Measurements

Tor A. Johansen, Jakob M. Hansen, Thor I. Fossen

Center for Autonomous Marine Operations and Systems (AMOS), Dept. Engineering Cybernetics,
Norwegian University of Science and Technology, Trondheim, Norway.
Email: tor.arne.johansen@itk.ntnu.no, thor.fossen@ntnu.no

A modular nonlinear observer for inertial navigation aided by pseudo-range measurements is designed and analyzed. The attitude observer is based on a recent nonlinear complementary filter that uses magnetometer and accelerometer vector measurements to correct the quaternion attitude estimate driven by gyro measurements, including gyro bias estimation. A tightly integrated translational motion observer is driven by accelerometer measurements, employs the attitude estimates, and makes corrections using the pseudo-range and range-rate measurements. It estimates position, range bias errors, velocity and specific force in an Earth-fixed Cartesian coordinate frame, where the specific force estimate is used as a reference vector for the accelerometer measurements in the attitude observer. The exponential stability of the feedback interconnection of the two observers is analyzed and found to have a semi-global region of attraction with respect to attitude observer initialization, and local region of attraction with respect to translational motion observer initialization. The latter is due to linearization of the range measurement equations that is underlying the selection of injection gains by solving a Riccati equation. In typical applications the pseudo-range equations admit an explicit algebraic solution that can be easily computed and used to accurately initialize the position and velocity estimates. Hence, the limited region of attraction is not seen as a practical limitation of the approach. Advantages of the proposed nonlinear observer are low computational complexity and a solid theoretical foundation.

1 Introduction

Range measurement is the basis for global satellite navigation systems, hydro-acoustic positioning systems, terrestrial radio navigation, and other positioning systems. Such systems commonly detect the time-of-arrival (TOA) of signals encoded in electromagnetic or acoustic waves to estimate the range, and are therefore prone to systematic errors such as clock synchronization errors or uncertain wave propagation speed. Since they do not directly measure the true

geometric range, they are often called pseudo-range measurements.

Inertial sensors such as accelerometer and gyros can be used to estimate position and velocity by integrating the kinematic equation. Since biases and other errors are accumulated in this process, leading to unbounded errors on the estimates, inertial navigation systems are usually aided by range measurements that can be used to stabilize these errors using a state estimator. There are two main design philosophies for these such estimators: Loosely and tightly coupled integration, [1–3]. In a loosely integrated scheme, a standalone estimator for position and velocity in an Earth-fixed Cartesian reference coordinate frame is first made using only the pseudo-range measurements. These position and velocity estimates are in turn used as measurements in a state observer that integrates them with the inertial measurements. In a tightly integrated scheme, the pseudo-range measurements are used directly in the state observer together with the inertial measurements. While the advantage of loosely coupled integration is a high degree of modularity, the advantage of tight integration is increased accuracy and fault tolerance, in particular in situations with highly accelerated vehicles and few range measurements, weak or noisy signals, unknown wave propagation delays, poor transponder geometry, or other anomalies, e.g. [1, 2]. More accurate models of measurement errors can be used in the integration filter and a reduced number of pseudo-range measurements can be used for aiding when a standalone position estimate cannot be determined, [1–3].

The state-of-the-art method for real-time fusion of the data from the individual sensors are nonlinear versions of the Kalman-filter (KF), [1, 2, 4], including the extended KF, unscented KF, particle filter, and specially tailored variants such as the multiplicative KF for attitude estimation using quaternions, [5, 6]. While the KF is a general method that has found extremely wide applicability, it has some drawbacks. This includes the relatively high computational cost and a rather implicit and not so easily verifiable convergence

properties that may require advanced supervisory functions and accurate initialization, [7]. Its major advantages are flexibility in tuning and application, as it is a widely known and used technology with intuitive and physically motivated tuning parameters interpreted as noise covariances, and providing certain optimality guarantees.

Our objective is to develop a low-complexity nonlinear observer for inertial navigation aided by a magnetometer and pseudo-range measurements, where the observer has properties founded on stability theory. The nonlinear observer structure is inspired by [8], where a loose integration between GNSS position/velocity measurements and inertial measurements was derived with semiglobal asymptotic stability conditions. Its extension to tightly integrated inertial navigation is non-trivial since the measurement equations are nonlinear when considering pseudo-range and range-rate measurements for aiding, instead of being linear when position and velocity estimates in an Earth-fixed Cartesian coordinate frame are used for aiding.

A similar research objective is pursued in the series of articles represented by [9–14]. Using a state transformation and a state augmentation they derive a linear time-varying (LTV) model which is closely related to the nonlinear model, and use this for the design of an estimator for attitude, position and velocity using hydro-acoustic range measurements. In contrast, our objective is to avoid unnecessary computational complexity.

We base the design philosophy on the assumption that the line-of-sight (LOS) vectors between the vehicle and the used transponders¹ are relatively slowly time-varying. This is a good assumption in many practical situations, such as terrestrial navigation using satellites, and surface ship positioning in deep waters using hydro-acoustic transponders at the seabed. In this case, time-varying observer gains multiplying pseudo-range and range-rate errors in the injection terms can be designed to shape the dynamics of the observer using a time-varying linearized relationship between range and vehicle position. Using the semiglobally exponentially stable nonlinear attitude observer of [15], see also [8, 16], we do not use a KF in the observer, but a slowly time-varying Riccati equation for gain matrix updates to the translational motion observer is employed. This allows the integration of the Riccati equation to be performed on a slower time-scale corresponding to the relative geometric configuration of the transponders and the receiver, or even solved periodically at low rate as an algebraic Riccati equation. This ensures low computational complexity, and a rigorous analysis of the observer error dynamics stability is made in the paper.

1.1 Outline

The paper is organized as follows: Models and preliminaries are described in section 2. This includes existence, uniqueness and computation of algebraic solution to the pseudo-range equations. In section 3 we present observers for attitude and translational motion, and analyze the

stability of their interconnections. The method is compared to a multiplicative EKF using experimental pseudo-range measurements to illustrate the methods in section 4 before conclusions are made in section 5. A short and preliminary version of this paper is presented in [17].

1.2 Notation

We use $\|\cdot\|_2$ for the Euclidean vector norm, $\|\cdot\|$ for the induced matrix norm, and denote by $(z_1; z_2)$ the column vector with the vector z_1 stacked over the vector z_2 . We denote by I_n the identity matrix of dimension n , and we use 0 to symbolize a matrix of zeros, where the dimensions are implicitly given by the context. For simplicity of notation, we usually let time dependence be implicit.

A unit quaternion $q = (s_q; r_q)$ with $\|q\|_2 = 1$ consists of a scalar part $s_q \in \mathbb{R}$ and a vector part $r_q \in \mathbb{R}^3$. For a vector $x \in \mathbb{R}^3$ we denote by \bar{x} the quaternion with zero real part and vector part x , i.e. $\bar{x} = (0; x)$. The conjugate of a quaternion q is denoted q^* , and the product of two quaternions is the Hamilton quaternion product. For a vector $x \in \mathbb{R}^3$ we define the skew-symmetric matrix

$$S(x) = \begin{pmatrix} 0 & -x_3 & x_2 \\ x_3 & 0 & -x_1 \\ -x_2 & x_1 & 0 \end{pmatrix}$$

We may use a superscript index to indicate the coordinate system in which a given vector is decomposed, thus x^a and x^b refers to the same vector decomposed in the coordinated systems indexed by a and b , respectively. The rotation from coordinate frame a to coordinate frame b may be represented by a quaternion q_a^b . The corresponding rotation matrix is denoted $R(q_a^b)$. The rate of rotation of the coordinate system indexed by b with respect to a , decomposed in c , is denoted ω_{ab}^c . We use e for the Earth-Centered Earth-Fixed (ECEF) coordinate system, b for the vehicle BODY-fixed coordinate system, and i for the Earth-Centered Inertial (ECI) coordinate system.

2 Models and preliminaries

2.1 Vehicle kinematics

The vehicle model is given by

$$\dot{p}^e = v^e \tag{1}$$

$$\dot{v}^e = -2S(\omega_{ie}^e)v^e + f^e + g^e(p^e) \tag{2}$$

$$\dot{q}_b^e = \frac{1}{2}q_b^e\bar{\omega}_{ib}^b - \frac{1}{2}\bar{\omega}_{ie}^e q_b^e \tag{3}$$

where $p^e, v^e, f^e \in \mathbb{R}^3$ are position, linear velocity and specific force in ECEF, respectively. The attitude of the vehicle is represented by a unit quaternion q_b^e . It represents the rotation from BODY to ECEF, and ω_{ib}^b represents the rotation rate of BODY with respect to ECI. The known vector ω_{ie}^e represents the Earth's rotation rate about the ECEF z -axis, and $g^e(p^e)$ denotes the plumb-bob gravity vector.

¹Note that we use the term transponder as a general concept that also includes navigation satellites in space, for example.

2.2 Measurement models

The inertial sensor model is based on the strapdown assumption, i.e. the IMU is fixed to the BODY frame and gives measurements $f_{IMU}^b = f^b$ and $\omega_{ib,IMU}^b = \omega_{ib}^b + b^b$ where $b^b \in \mathbb{R}^3$ denotes the rate gyro bias that is assumed to satisfy $\|b^b\|_2 \leq M_b$ for some known bound M_b and is slowly time-varying:

$$\dot{b}^b = 0 \quad (4)$$

It is further assumed that any accelerometer bias and drift is compensated for. The magnetometer measures the direction of the 3-dimensional Earth magnetic vector field $m_{mag}^b = m^b$.

Range measurements are typically generated by measuring the TOA of known signal waveforms (acoustic or electromagnetic). Due to errors in clock synchronization and wave propagation velocity, such measurements often contain systematic errors (biases) in addition to random errors, e.g. [18], and must therefore be treated as pseudo-range measurements. The range measurement model is

$$y_i = \rho_i + \zeta_i^T \beta, \quad \rho_i = \|p^e - p_i^e\|_2 \quad (5)$$

for $i = 1, 2, \dots, m$ where y_i is a (pseudo-)range measurement, p_i^e is the known position of the i -th transponder, m is the number of transponders, ρ_i is the geometric range, $\beta \in \mathbb{R}^n$ is a vector of range error model parameters (biases) to be estimated, and the coefficient vector ζ_i describes the influence of each element of β on pseudo-range measurement y_i . This framework allows both individual and common mode slowly time-varying errors such as receiver clock bias (i.e. $\zeta_i = 1$ and $\beta := c\Delta_c$ where Δ_c is the clock bias and c is the wave speed) or wave propagation delays to be taken into account:

$$\dot{\beta} = 0 \quad (6)$$

Note that $\dot{\beta} = 0$ is the classical constant parameter assumption in adaptive estimation and does not prevent us from estimating a slowly time-varying β in practice.

Range-rate measurements are usually found by considering Doppler-shift or tracking of features or codes in signals. Also here there may be systematic (bias) errors in some cases, depending on the sensor principle and technology. The range-rate (speed) measurement model is given by

$$v_i = \frac{1}{\rho_i} (p^e - p_i^e)^T (v^e - v_i^e) + \varphi_i^T \beta \quad (7)$$

where v_i is the relative range-rate measurement, the coefficient vector φ_i describes the effect of each element of β on range speed measurement v_i , and we define $v_i^e := \dot{p}_i^e$. Eq. (7) follows from time-differentiation of (5), assuming an independent error model. Hence, we use the term $\varphi_i^T \beta$ instead of $\zeta_i^T \dot{\beta}$ in (7) since it provides additional flexibility in modeling.

2.3 Algebraic range and pseudo-range solutions

Despite the nonlinear form of the pseudo-range measurement equation (5), we can use its quadratic structure to get a relatively simple algebraic solution, [18–21]. Assume an arbitrary reference position \hat{p}^e is given, and define LOS vectors $\check{p}_i^e := \hat{p}^e - p_i^e$ for every i . The following explicit procedure can be used to determine a position estimate.

Lemma 1. *Assume we have available pseudo-range measurements y_1, y_2, y_3 , and y_4 where the three first transponder line-of-sight vectors among $\check{p}_1^e, \check{p}_2^e, \check{p}_3^e$, and \check{p}_4^e are linearly independent, and*

$$y_4 \neq (y_1, y_2, y_3) \check{A}^{-1} \check{p}_4^e \quad (8)$$

where $\check{A} = (\check{p}_1^e \check{p}_2^e \check{p}_3^e)$ Assume $\zeta_i = 1$ for all $i = 1, 2, 3, 4$ (i.e. a single common mode error parameter $\beta \in \mathbb{R}$), then $p^e = \hat{p}^e + \check{p}^e$ is derived from $z = (\check{p}^e; \beta)$ where

$$z = \frac{\check{r}\check{u} + \check{v}}{2}, \quad \check{u} = \hat{A}^{-T} \check{e}, \quad \check{v} = \hat{A}^{-T} \check{b}$$

$$\check{r} = \frac{-2 - \check{u}^T M \check{v} \pm \sqrt{(2 + \check{u}^T M \check{v})^2 - \check{u}^T M \check{u} \cdot \check{v}^T M \check{v}}}{\check{u}^T M \check{u}}$$

where $\check{e} = (1; 1; 1; 1)$, $\check{b} \in \mathbb{R}^4$ has components $\check{b}_i = y_i^2 - \|\check{p}_i^e\|_2^2$, $M = \text{diag}(1, 1, 1, -1)$, and

$$\hat{A} = \begin{pmatrix} \check{p}_1^e & \check{p}_2^e & \check{p}_3^e & \check{p}_4^e \\ y_1 & y_2 & y_3 & y_4 \end{pmatrix}$$

Proof. The proof is similar to those found in [18–21]. \square

The computations are analytic and the most complex operations are the inversion of a 4×4 -matrix as well as the square-root computation. We note that there are in general two solutions. This ambiguity can be solved in several ways. For example, by using five or more pseudo-range measurements, the problem can be solved directly from a linear equation, cf. [18–21]. Ambiguity may also be resolved using domain knowledge. One example is terrestrial navigation when there is a large distance to the navigation satellites such that non-terrestrial solutions for the vehicle position can be ruled out. Another example is underwater navigation where all transponders are located on the seabed and the vehicle is at the surface or at some distance from the seabed such that positions below the seabed can be ruled out. Additional sensors for e.g. depth or altitude can also be used directly to select the correct solution.

Remark 1. *The velocity can be estimated by solving a linear problem by inserting the position and bias parameter estimates in the measurement equation (7).*

Remark 2. *If the condition (8) does not hold, the null-space of \hat{A} is given by $y_4 \beta + (y_1, y_2, y_3) \check{p}_4^e = 0$. Solutions for p^e may be estimated by fixing β , or solved using another measurement if available.*

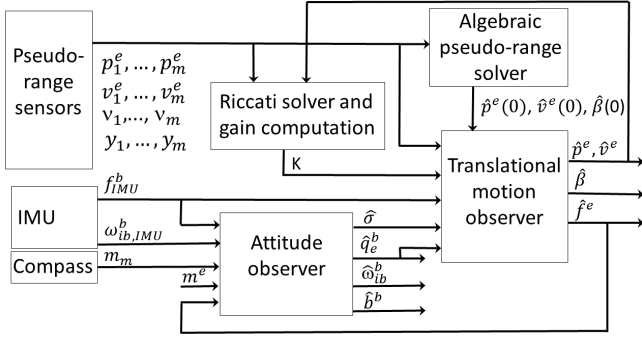


Fig. 1. Observer block diagram.

Remark 3. With an error model that requires a vector $\beta \in \mathbb{R}^n$ rather than a scalar β , the solution may require more than 4 measurements and up to n coupled quadratic equations to be solved, possibly leading to additional ambiguity.

In typical range-measurements systems, the remaining measurement errors are typically so small that a good position and velocity initialization of an observer can be found using Lemma 1 such that a relatively small region of attraction with respect to position, velocity and bias parameter initialization error can be accepted.

We have chosen to consider only the effect of slowly time-varying systematic errors (parameterized by β), such as biases, in this presentation and analysis. Rapidly varying errors such as noise can possibly be handled by appropriate tuning of the gains and may not influence the structure of the observer. In some cases, better estimation accuracy can be achieved by further modeling of the errors using e.g. Markov-like models, which are straightforward to include in the proposed framework by augmenting the translational motion observer with the new states.

3 Nonlinear observer

The overall structure of the observer is given in Figure 1. Sections 3.1 and 3.2 describes the two main modules, i.e. the attitude observer and the translational motion observer. In addition, the initialization based on the algebraic pseudo-range solver was presented in Section 2.3, and the Riccati solution and gain computation in Section 3.3.

3.1 Attitude observer

We use the attitude observer from [15, 16]

$$\dot{\hat{q}}_b^e = \frac{1}{2} \hat{q}_b^e \left(\bar{\omega}_{ib,IMU}^b - \bar{b}^b + \hat{\sigma} \right) - \frac{1}{2} \bar{\omega}_{ie}^e \hat{q}_b^e \quad (9)$$

$$\hat{b}^b = \text{Proj} \left(-k_f \hat{\sigma}, \|\hat{b}^b\|_2 \leq M_b \right) \quad (10)$$

$$\hat{\sigma} = k_1 m_{mag}^b \times R(\hat{q}_b^e)^T m^e + k_2 f_{IMU}^b \times R(\hat{q}_b^e)^T \text{sat}_{M_f}(\hat{f}^e) \quad (11)$$

where ω_{ie}^e and m^e are assumed known. $\text{Proj}(\cdot)$ is a projection operator that ensures $\|\hat{b}^b\|_2 \leq M_b$ with $M_b > M_b$, see [8]. Moreover, $\text{sat}_{M_f}(\cdot)$ is a saturation operator, with M_f such that $\|f^e\|_2 \leq M_f$. The QUEST algorithm, [22], may be used for initialization of the attitude.

The estimation error is defined as $\tilde{q} = q_b^e \hat{q}_b^{e*}$ and $\tilde{b} = b^b - \hat{b}^b$, and we define $\chi = (\tilde{s}; \tilde{b})$ where \tilde{s} denotes the scalar part of the quaternion \tilde{q} . Semiglobal stability of the origin $\chi = 0$ of the error dynamics of the attitude observer can be established under the following observability assumption:

Assumption 1. The acceleration f^b and its rate \dot{f}^b are uniformly bounded, and there exist a constant $c_{obs} > 0$ such that $\|f^b \times m^b\|_2 \geq c_{obs}$ for all $t \geq 0$.

Initial conditions are restricted to the following sets:

Assumption 2. $\hat{q}_b^e(0) \in \mathcal{D}(\bar{\epsilon})$, where $\mathcal{D}(\bar{\epsilon}) = \{\tilde{q} \mid \tilde{s} > \bar{\epsilon}\}$ represents a set of attitude errors bounded away from 180° by a margin determined by an arbitrary constant $\bar{\epsilon} \in (0, \frac{1}{2})$. Moreover, $\hat{b}^e(0) \in \mathcal{B} = \{b \in \mathbb{R}^3 \mid \|b\|_2 \leq M_b\}$.

Lemma 2. Assume $\hat{f}^e = f^e$. Then for each $\epsilon \in (0, \frac{1}{2})$ there exists a $k_p^* > 0$ such that if $k_1, k_2 > k_p^*$ and $k_I > 0$ then

$$\|\chi(t)\|_2 \leq \kappa_a e^{-\lambda_a t} \|\chi(0)\|_2 \quad (12)$$

for some $\kappa_a, \lambda_a > 0$.

Proof. See [8]. \square

3.2 Translational motion observer

We propose the following observer

$$\dot{\hat{p}}^e = \hat{v}^e + \sum_{i=1}^m (K_i^{pp} e_{y,i} + K_i^{pv} e_{v,i}) \quad (13)$$

$$\dot{\hat{v}}^e = -2S(\omega_{ie}^e) \hat{v}^e + \hat{f}^e + g^e(\hat{p}^e) + \sum_{i=1}^m (K_i^{vp} e_{y,i} + K_i^{vv} e_{v,i}) \quad (14)$$

$$\dot{\hat{\xi}} = -R(\hat{q}_b^e) S(\hat{\sigma}) f_{IMU}^b + \sum_{i=1}^m (K_i^{\xi p} e_{y,i} + K_i^{\xi v} e_{v,i}) \quad (15)$$

$$\hat{f}^e = R(\hat{q}_b^e) f_{IMU}^b + \hat{\xi} \quad (16)$$

$$\dot{\hat{\beta}} = \sum_{i=1}^m (K_i^{\beta p} e_{y,i} + K_i^{\beta v} e_{v,i}) \quad (17)$$

where the gain matrices K_i^* are in general time-varying. While the structure is similar to [8], the injection terms are different, and [8] does not include estimation of parameters β . A common feature is that f^e is viewed as an unknown input, which is estimated in (15)–(16) to be used in (11). The injection errors from pseudo-range and range-rate measurements are defined as $e_{y,i} := y_i - \hat{y}_i$ and $e_{v,i} := v_i - \hat{v}_i$, with estimated measurements

$$\hat{y}_i = \hat{\rho}_i + \zeta_i^T \hat{\beta}, \quad \hat{v}_i = \left(\frac{\hat{p}^e - p_i^e}{\hat{\rho}_i} \right)^T (\hat{v}^e - v_i^e) + \phi_i^T \hat{\beta}$$

where $\hat{\rho}_i := \|\hat{p}^e - p_i^e\|_2$, and the estimation errors are $\tilde{p} := p^e - \hat{p}^e$, $\tilde{v} := v^e - \hat{v}^e$, and $\tilde{\beta} := \beta - \hat{\beta}$. Next, we consider a linearization of the injection terms.

Assumption 3. *At all time, $\bar{\rho} \geq \rho_i \geq \underline{\rho} > 0$.*

Assumption 4. *At all time, $\|v^e - v_i^e\|_2 \leq \bar{v}$.*

Assumption 5. *The transponder positions p_i^e and their velocities v_i^e are known.*

Lemma 3. *The injection errors satisfy*

$$e_{y,i} = \left(\frac{\hat{p}^e - p_i^e}{\hat{\rho}_i} \right)^T \tilde{p} + \zeta_i^T \tilde{\beta} + \varepsilon_{y,i} \quad (18)$$

$$e_{v,i} = \left(\frac{\hat{v}^e - v_i^e}{\hat{\rho}_i} \right)^T \tilde{p} + \left(\frac{\hat{p}^e - p_i^e}{\hat{\rho}_i} \right)^T \tilde{v} + \varphi_i^T \tilde{\beta} + \varepsilon_{v,i} \quad (19)$$

where

$$\|\varepsilon_{y,i}\|_2 \leq \frac{1}{\underline{\rho}} \|\tilde{p}\|_2^2 \quad (20)$$

$$\|\varepsilon_{v,i}\|_2 \leq \frac{1}{\underline{\rho}} \|\tilde{p}\|_2 \cdot \|\tilde{v}\|_2 + \frac{3\bar{v}}{2\underline{\rho}^2} \|\tilde{p}\|_2^2 \quad (21)$$

Proof. See Appendix A. \square

We define the state of the error dynamics as $x := (\tilde{p}; \tilde{v}; \tilde{\beta})$, where $\tilde{f} := f^e - \hat{f}^e$ replaces ξ as a state by combining (15) and (16). Summarized, the equations for the predicted measurement error can now be written in the linearized time-varying form

$$e_{y,i} = C_{y,i}x + \varepsilon_{y,i} \quad (22)$$

$$e_{v,i} = C_{v,i}x + \varepsilon_{v,i} \quad (23)$$

where the $2m$ rows $C_{y,i}$ and $C_{v,i}$ of the time-varying matrix $C := (C_{y,1}; \dots; C_{y,m}; C_{v,1}; \dots; C_{v,m})$ are defined by $C_{y,i} := (d_i^T, 0, 0, \zeta_i^T)$ and $C_{v,i} := (\tilde{v}_i^T, d_i^T, 0, \varphi_i^T)$. The estimated line-of-sight vectors are $\tilde{d}_i := (\hat{p}^e - p_i^e)/\hat{\rho}_i = \tilde{p}_i^e/\hat{\rho}_i$ and the normalized estimated relative velocity vectors are $\tilde{v}_i := (\hat{v}^e - v_i^e)/\hat{\rho}_i$, for $i = 1, 2, \dots, m$. We note that

$$C = \begin{pmatrix} G^T & 0 & 0 & D_p^T \\ B^T & G^T & 0 & D_v^T \end{pmatrix}$$

where $G = (\check{p}_1^e, \dots, \check{p}_m^e) \in \mathbb{R}^{3 \times m}$, $B = (\check{v}_1^e, \dots, \check{v}_m^e) \in \mathbb{R}^{3 \times m}$, and $D = (D_p, D_v)$ with $D_p = (\zeta_1, \dots, \zeta_m)$ and $D_v = (\varphi_1, \dots, \varphi_m)$.

We note that the time-varying matrix C is known at the current time and can be used for selection of gains. We also observe that in typical applications with large distance between the vehicle and transponders, their relative positions and line-of-sight vectors will be slowly time-varying,

and hence the measurement matrix C will be slowly time-varying, since due to Lemma 1 the transients resulting from initialization of position and velocity are not expected to be significant. Following similar steps as in [8], we arrive at the error dynamics

$$\dot{x} = (A - KC)x + \rho_1(t, x) + \rho_2(t, \chi) + \rho_3(t, x) \quad (24)$$

where

$$A := \begin{pmatrix} 0 & I_3 & 0 & 0 \\ 0 & 0 & I_3 & 0 \\ 0 & 0 & 0 & 0 \\ 0 & 0 & 0 & 0 \end{pmatrix}, \quad K := \begin{pmatrix} K_1^{pp} & \dots & K_m^{pp} & K_1^{pv} & \dots & K_m^{pv} \\ K_1^{vp} & \dots & K_m^{vp} & K_1^{vv} & \dots & K_m^{vv} \\ K_1^{\xi p} & \dots & K_m^{\xi p} & K_1^{\xi v} & \dots & K_m^{\xi v} \\ K_1^{\beta p} & \dots & K_m^{\beta p} & K_1^{\beta v} & \dots & K_m^{\beta v} \end{pmatrix}$$

The perturbation terms are defined as $\rho_1(t, x) := (0; \rho_{12}(t, x); 0; 0)$ with $\rho_{12}(t, x) = -2S(\omega_{ie}^e)x_2 + (g^e(p^e) - g^e(p^e - x_1))$ and $\rho_2(t, \chi) := (0; 0; \tilde{d}; 0)$ with

$$\begin{aligned} \tilde{d} = & (I - R(\tilde{q})^T)R(q_b^e)(S(\omega_{ib}^b)f^b + \dot{f}^b) \\ & - S(\omega_{ie}^e)(I - R(\tilde{q})^T)R(q_b^e)f^b - R(\tilde{q})^T R(q_b^e)S(\tilde{b})f^b \end{aligned}$$

In [8] it is shown that $\|\rho_2(t, \chi)\|_2 \leq \gamma_3 \|\chi\|_2$ for some constant $\gamma_3 > 0$. A fundamental difference compared to [8] is that the matrix C is time-varying (rather than constant), and there is an additional perturbation term $\rho_3(t, x) := K\varepsilon(t, x)$ that results from the linearization of the injection terms: $\varepsilon := (\varepsilon_{y,1}; \dots; \varepsilon_{y,m}; \varepsilon_{v,1}; \dots; \varepsilon_{v,m})$. We note that from Lemmas 1 and 3 that ε is small when $\underline{\rho}$ is large compared to $\|\tilde{p}\|_2$, $\|\tilde{v}\|_2$ and \bar{v} . Compared to [8] this means that a different strategy for selection of gains is needed, and one can not hope for a global stability result. Nevertheless, as in [8], we want to employ a constant parameter $\theta \geq 1$ in order to assign a certain time-scale structure to the error dynamics (24). For this purpose, we introduce the non-singular state-transform matrix

$$L_\theta := \text{blockdiag} \left(I_3, \frac{1}{\theta} I_3, \frac{1}{\theta^2} I_3, \frac{1}{\theta^3} I_n \right) \quad (25)$$

and the state transform $\eta = L_\theta x$.

Lemma 4. *Let $K_0 \in \mathbb{R}^{(9+n) \times 2m}$ be an arbitrary time-varying gain matrix, and $\theta \geq 1$ be an arbitrary constant. Define*

$$K := \theta L_\theta^{-1} K_0 E_\theta \quad (26)$$

and assume the time-varying $E_\theta \in \mathbb{R}^{2m \times 2m}$ satisfies $E_\theta C = CL_\theta$. Then the error dynamics (24) is equivalent to

$$\begin{aligned} \frac{1}{\theta} \dot{\eta} = & (A - K_0 C)\eta + \frac{1}{\theta} \rho_1(t, \eta) + \frac{1}{\theta^3} \rho_2(t, \chi) \\ & + K_0 E_\theta \varepsilon(t, L_\theta^{-1} \eta) \end{aligned} \quad (27)$$

Proof. The transformed dynamics are derived by substituting (24) in $\dot{\eta} = L_\theta \dot{x}$. It is straightforward to show that the structure of A leads to $L_\theta A x = \theta A \eta$. Moreover,

$$L_\theta K C x = \theta L_\theta L_\theta^{-1} K_0 E_\theta C x = \theta K_0 C L_\theta x = \theta K_0 C \eta$$

The rest of the proof follows by change of variables according to $\eta = L_\theta x$. \square

The existence of an E_θ satisfying $E_\theta C = C L_\theta$ depends on the null-space of C , as shown next.

Assumption 6. i) The number of transponders is $m \geq 3 + \lceil k/2 \rceil$, where $k = \text{rank}(D^T)$. ii) 3 of the estimated line-of-sight vectors are linearly independent, i.e. $\text{rank}(G) = 3$. iii) 3 of the estimated normalized relative velocity vectors are linearly independent, i.e. $\text{rank}(B) = 3$.

Lemma 5. $E_\theta = C L_\theta C^+$ satisfies $E_\theta C = C L_\theta$, where C^+ is the Moore-Penrose right pseudo-inverse of C .

Proof. See Appendix A. \square

The assumption is reasonable and closely related to the assumptions underlying Lemma 1, as well as observability that will be considered shortly. If there are no range-rate measurements, it can be verified that condition i) can be replaced by $m \geq 3 + k$.

3.3 Stability analysis

As the first step towards the stability analysis, we consider the LTV nominal error dynamics

$$\frac{1}{\theta} \dot{\eta} = (A - K_0 C) \eta \quad (28)$$

and analyze its stability and robustness before we consider the effect of the perturbations in (27).

Let $R > 0$ be a symmetric matrix that can be interpreted as the covariance of the pseudo-range and range-rate measurement noises. The observability Gramian for the system $(A, R^{-1/2} C)$ is

$$\mathcal{W}(t, t + \tau) = \int_t^{t+\tau} \Phi^T(T) C^T(T) R^{-1} C(T) \Phi(T) dT$$

where the transition matrix is $\Phi(T) = e^{AT}$, and we recall (from e.g. [23]) that the LTV system is said to be uniformly completely observable if there exist constants $\alpha_1, \alpha_2, \tau > 0$ such that for all $t \geq 0$ we have $\alpha_1 I \leq \mathcal{W}(t, t + \tau) \leq \alpha_2 I$.

Assumption 7. The LTV system $(A, R^{-1/2} C)$ is completely uniformly observable.

Remark 4. Assumption 7 is related to Assumption 6, as well as the conditions of Lemma 1. This is further discussed in Appendix B.

There may be many ways to choose a time-varying gain matrix K_0 such that (28) has desired performance and stability. A straightforward approach with considerable flexibility for tuning is to use a Riccati-equation similar to the gain of a Kalman-Bucy filter for the system (A, C) as described below. In this case, the close relationship between the complete uniform observability conditions and the boundedness of the covariance matrix estimate P is well known, e.g. [7], and can be monitored in real-time without much additional computations.

Assumption 8. C is uniformly bounded.

Remark 5. It can be observed that the only terms in C that may not be uniformly bounded are of the form $(\hat{v}^e - v_i^e)/\hat{\rho}_i$. Thus, unbounded C may only occur if \hat{v} goes unbounded. While this can be dealt with in many ways, a simple approach is resetting of \hat{v}^e based of the velocity computed from raw range and range-rate measurements (cf. Lemma 1) if \hat{v}^e grows out of bounds.

Lemma 6. Let

$$K_0 := P C^T R^{-1} \quad (29)$$

where P satisfies the Riccati equation

$$\frac{1}{\theta} \dot{P} = A P + P A^T - P C^T R^{-1} C P + Q \quad (30)$$

for some positive definite symmetric matrices Q, R , and $P(0)$. Then P is uniformly bounded and the origin is a globally exponentially stable equilibrium point of the LTV nominal error dynamics (28) with any constant $\theta \geq 1$.

Proof. The proof follows from [23, 24], and we repeat the main ideas since we need the Lyapunov function later. Consider a Lyapunov function candidate $U(\eta, t) = \frac{1}{\theta} \eta^T P^{-1} \eta$, which is positive definite and well-defined due to the time-varying matrix P satisfying (30) being symmetric, positive definite with some margin, and bounded. It follows by standard arguments that along the trajectories of (28) and (30) that $\dot{U} = -\eta^T (P^{-1} Q P^{-1} + C^T R^{-1} C) \eta$ and the result follows by the positive definiteness of P^{-1} and Q . \square

The structure of the observer is illustrated in the block diagram in Figure 1. We notice two feedback loops where one is due to the use of \hat{f}^e as a reference vector in the attitude observer and the other is caused by linearization of the pseudo-range measurement equations to get the C -matrix in (29) and (30).

Initialization of position and velocity is based on the algebraic solution, cf. Lemma 1. If the vehicle is not strongly accelerated during initialization, then also the specific force initialization can be made accurately with $\xi(0) = 0$ that gives $\hat{f}^e(0) = R(\hat{q}_b^e(0)) f_{IMU}^b(0)$. Below, we analyze the conditions for exponential stability.

Assumption 9. Initial conditions are in the following sets:

1. $\mathcal{X} \subset \mathbb{R}^{9+n}$ is a ball containing the origin.
2. $\mathcal{P} \subset \mathbb{R}^{(9+n) \times (9+n)}$ is an arbitrary compact set of symmetric positive definite matrices.
3. $\mathcal{D}(\bar{\epsilon}) = \{\tilde{q} \mid \tilde{s} > \bar{\epsilon}\}$ represents a set of attitude errors bounded away from 180° by a (small) margin determined by an arbitrary constant $\bar{\epsilon} \in (0, \frac{1}{2})$.
4. $\mathcal{B} = \{b \in \mathbb{R}^3 \mid \|b\|_2 \leq M_b\}$.

Assumption 10. Observer gains are chosen according to

1. $k_1, k_2 > 0$ are sufficiently large, cf. [8].
2. $k_I > 0$ is arbitrary.
3. K is chosen according to (26), (29) and (30) tuned by symmetric $Q, R > 0$.

Proposition 1. There exists a $\theta^* \geq 1$ such that for all $\theta \geq \theta^*$, P is uniformly bounded and

$$\sqrt{\|x(t)\|_2^2 + \|\chi(t)\|_2^2} \leq \kappa e^{-\lambda t} \sqrt{\|x(0)\|_2^2 + \|\chi(0)\|_2^2}$$

for some $\kappa > 0$ and $\lambda > 0$.

Proof. Using $U(\eta, t) := \frac{1}{\theta} \eta^T P^{-1} \eta$, we get from the proof of Lemma 6 that

$$\begin{aligned} \dot{U} &= -\eta^T (P^{-1} Q P^{-1} + C^T R^{-1} C) \eta + \frac{2}{\theta} \eta^T P^{-1} \rho_1(t, \eta) \\ &\quad + \frac{2}{\theta} \eta^T P^{-1} P C^T R^{-1} E_\theta \epsilon + \frac{2}{\theta^3} \eta^T P^{-1} \rho_2(t, \chi) \\ &\leq -\gamma_1 \|\eta\|_2^2 + \frac{2}{\theta} \|\eta\|_2 \cdot \|C^T R^{-1}\| \cdot \sum_{i=1}^m \|E_\theta\| (\epsilon_{y,i}^2 + \epsilon_{r,i}^2) \\ &\quad + \frac{1}{\theta} \gamma_2 \gamma_4 \|\eta\|_2^2 + \frac{1}{\theta^3} \gamma_3 \gamma_4 \|\eta\|_2 \cdot \|\chi\|_2 \end{aligned}$$

where $\gamma_1, \gamma_2, \gamma_3, \gamma_4 > 0$ are constants independent of θ . Note that a uniform bound on P^{-1} that does not depend on θ is established in Lemma 6 in [17]. Next, using Lemma 3, we have

$$\begin{aligned} \dot{U} &\leq -\gamma_1 \|\eta\|_2^2 + \frac{1}{\theta} \gamma_5(\underline{\rho}, \bar{\nu}) \|\eta\|_2^3 \\ &\quad + \frac{1}{\theta} \gamma_2 \gamma_4 \|\eta\|_2^2 + \frac{1}{\theta^3} \gamma_3 \gamma_4 \|\eta\|_2 \cdot \|\chi\|_2 \end{aligned}$$

where $\gamma_5(\underline{\rho}, \bar{\nu})$ increases with $\bar{\nu}$ and decreases with $\underline{\rho}$, and is independent of θ .

Similar to [8], we can show that for any $\delta > 0$ and $T > 0$ there exists a $\theta_1^* \geq 1$ such that for $\theta \geq \theta_1^*$ there exists an invariant set $\mathcal{X}_1 \subset \mathbb{R}^{9+n}$ such that for $\|\eta(0)\|_2 \in \mathcal{X}_1$ we have for all $t \geq T$ that $\|\eta\|_2 \leq \delta$. As argued in [8] this implies $|\tilde{s}| \geq \bar{\epsilon}$ such that \tilde{q} never leaves $\mathcal{D}(\bar{\epsilon})$. Inspired by [8], we now define the function

$$W(t, \tilde{r}, \tilde{s}, \tilde{b}) := (1 - \tilde{s}^2) + 2\ell \tilde{s} \tilde{r} R(q_b^e) \tilde{b} + \frac{\ell}{k_I} \tilde{b}^T \tilde{b}$$

where $\ell > 0$ is a constant [16]. Under the condition $|\tilde{s}| \geq \bar{\epsilon}$, W is shown in [8] to satisfy

$$\dot{W} \leq -\gamma_7 \|\chi\|_2^2 + \gamma_6 \theta^2 \|\chi\|_2 \cdot \|\eta\|_2 \quad (31)$$

for some constants $\gamma_6, \gamma_7 > 0$ that are independent of θ . Next we define the Lyapunov-function candidate $V(t, \eta, \chi) := U(t, \eta) + \frac{1}{\theta^5} W(t, \chi)$. Then

$$\dot{V} \leq -z^T S(\theta) z + \frac{\gamma_5(\underline{\rho}, \bar{\nu})}{\theta} \|\eta\|_2^3$$

where we have defined the auxiliary state $z := (\|\eta\|_2; \|\chi\|_2) \in \mathbb{R}^2$, and the 2×2 -matrix

$$S(\theta) = \begin{pmatrix} \gamma_1 - \frac{\gamma_2 \gamma_4}{\theta} - \frac{\gamma_3 \gamma_4 + \gamma_6}{2\theta^3} & -\frac{\gamma_7}{\theta^5} \\ -\frac{\gamma_3 \gamma_4 + \gamma_6}{2\theta^3} & \frac{\gamma_7}{\theta^5} \end{pmatrix} \quad (32)$$

Considering the first-order and second-order principal minors of S , we get that $S(\theta^*) > 0$ if

$$\theta^* > \max \left(\frac{\gamma_2 \gamma_4}{\gamma_1}, \frac{\gamma_2 \gamma_4 \gamma_7 + (\gamma_3 \gamma_4 + \gamma_6)^2}{\gamma_1 \gamma_7} \right) \quad (33)$$

Hence, we can choose a $\theta^* \geq \theta_1^*$ satisfying (33) such that for all $\theta \geq \theta^*$ there exists an invariant set \mathcal{X}_2 and $\alpha_3, \alpha_4 > 0$, where for all $x \in \mathcal{X}_2$ we have

$$\dot{V} \leq -\alpha_3 \|z\|_2^2 - \alpha_4 \|\chi\|_2^2 \leq -2\lambda V$$

for some $\lambda > 0$, and the result follows by choosing \mathcal{X} as the largest invariant set such that $\mathcal{X} \subset \mathcal{X}_1 \cap \mathcal{X}_2$, and application of the comparison lemma, [25]. \square

Remark 6. The translational motion observer is not a KF since the state estimate update equation contains certain nonlinear terms and the auxiliary state ξ . It has the attractive feature that its error dynamics are accurately represented by a nominal LTV system that is used as a basis for selection of the injection gain matrices using the formulas for the Riccati-equation and gain matrix of the Kalman-Bucy filter.

Remark 7. In some cases when the parameter vector β influences all measurements in the same way, the variable β (or at least some of its elements) can be eliminated from the estimation problem by forming new measurements that are differences between original measurements. This is known as Time-Difference-of-Arrival (TDOA) measurements, e.g. [18, 21], and can be employed in order to further reduce the computational complexity of the estimator since an estimate of β is not needed for most applications.

Since the LTV system (27) is slowly time-varying, we can reap the benefits of solving the Riccati equation on a

slower time-scale than the estimator updates, roughly speaking only when there is a significant change in the transponders' LOS vectors due to the relative motion of the vehicle and the transponders, or enabling or disabling some range measurements. In many practical applications this can be implemented by solving the algebraic Riccati-equation periodically at low rate. In the context of terrestrial GNSS this relates to the dynamics of the satellites relative to the Earth, and in the context of a surface ship on dynamic positioning using hydro-acoustic positioning this relates to the motion of the ship relative to the transponders at the seabed. Hence, the proposed solution will in many typical applications not incur much more computations than a fixed-gain strategy and typically less than both a direct and indirect extended KF approach that would require updating of the covariance matrix at a higher update frequency.

4 Experimental Results

Experimental data is acquired using a Penguin B fixed-wing UAV equipped with a tactical grade IMU and GNSS receiver. The inertial and magnetometer measurement are available from an ADIS 16488 IMU at 410Hz, whereas pseudo-range and carrier-phase measurements are supplied by a u-Blox LEA-6T receiver at 5Hz. The pseudo-range measurements are corrected for time of transmission between satellite and receiver, as well as the tropospheric delay.

Additionally, a similar GNSS-receiver at a known and close location serves as a base station for a Real-Time-Kinematic (RTK) solution for the UAV position. The RTK position is determined using the open source program RTK-LIB, and will be used as reference since the RTK position is known to have decimeter-level accuracy, [3], since a fix or float solution is achieved at every time during the experiments. The flight trajectory is illustrated in Figure 2.

The nonlinear observer parameters are chosen as: $k_1 = 0.25$, $k_2 = 0.75$, $k_I = 0.004$, $R = 0.1^2 I_m$, $Q = \text{blockdiag}(0I_3, 10^{-10}I_3, 2.5 \cdot 10^{-4}I_3, 1)$.

A Multiplicative-Extended-Kalman-Filter (MEKF) is implemented for comparison. The MEKF integrates acceleration and angular velocity measured by the IMU with global ranges, see [5,6]. The attitude is represented as a unit quaternion, where the attitude increment \tilde{u} is included in the state vector resulting in 16 states, i.e. $x_{MEKF} = [\hat{p}^e; \hat{v}^e; \hat{f}^e; \tilde{u}; \hat{b}^b; \hat{\beta}]$. We note that the MEKF estimates \hat{f}^e to be used as an ECEF reference vector for the acceleration measurement in the attitude measurement model. The parameters for the MEKF are: $R_{MEKF} = \text{blockdiag}(0.1^2 I_m, 0.001I_3, 0.01I_3)$ where the six last elements correspond to the use of the magnetometer and accelerometer as aiding sensors for attitude, $Q_{MEKF} = \text{blockdiag}(0I_3, 10^{-10}I_3, 2.5 \cdot 10^{-4}I_3, 1, 10^{-5}I_3, 10^{-9}I_3)$.

It is interesting to note that the tuning of the TMO's of the nonlinear observers and the MEKF are compatible. The diagonal elements of the covariance matrices Q and R can be chosen based on the variances of the various measurements, and the same values can be used in the NLO and MEKF. This means that the nonlinear observer approach can take advantage of the extensive experiences with Kalman-filtering.

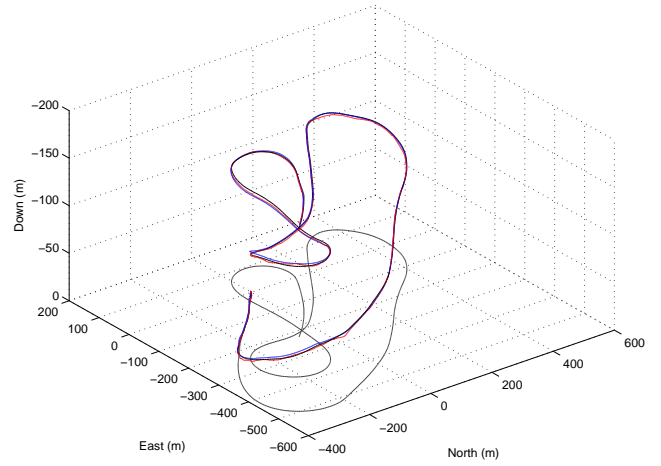


Fig. 2. Trajectory of the UAV.

4.1 Estimation accuracy

Experimental results where the position estimation error are shown for a part of the flight in Figures 3. The position estimation performance of the proposed nonlinear observer seen to be comparable to the MEKF, as shown in Table 1. Two versions of the nonlinear observer are compared, where the difference is related to the computation of the time-varying gain of the TMO: A discrete-time version where the TMO's Riccati-equation is updated at the 5 Hz GNSS frequency (denoted NLO) and a version where instead the algebraic Riccati-equation is solved periodically at 0.003 Hz (denoted NLO-ARE). It is easily seen that their estimates are very similar since the red and black curves are almost indistinguishable in Figure 3. Attitude estimates are shown in Figure 4.

We remark that improved estimates could possibly have been achieved by all methods by more realistic modeling of GNSS pseudo-range measurement errors using Markov-models. In order to keep the presentation and comparison simple, we have chosen not to include this extension in the present paper.

4.2 Computational load

The computational complexity of the proposed nonlinear observer is compared to the MEKF by counting the average number of arithmetic operations (additions and multiplications) per second in Table 2. These results show that the NLO and NLO-ARE computational loads are in average 23.6% and 21.6% of the MEKF, respectively.

The main difference in computational complexity is obviously related to the use of fixed gains in the nonlinear attitude observer. In addition, the TMO's multi-rate implementation of the gain computations and Riccati-equation solutions allows some computations to be saved. The MEKF implementation runs at GNSS frequency, i.e. 5 Hz. On the other hand, the two versions of the nonlinear observer updates the gains either by solving the Riccati equation at 5Hz (NLO) or an algebraic Riccati equation at 0.003Hz (NLO-ARE). The differences in estimation accuracy documented

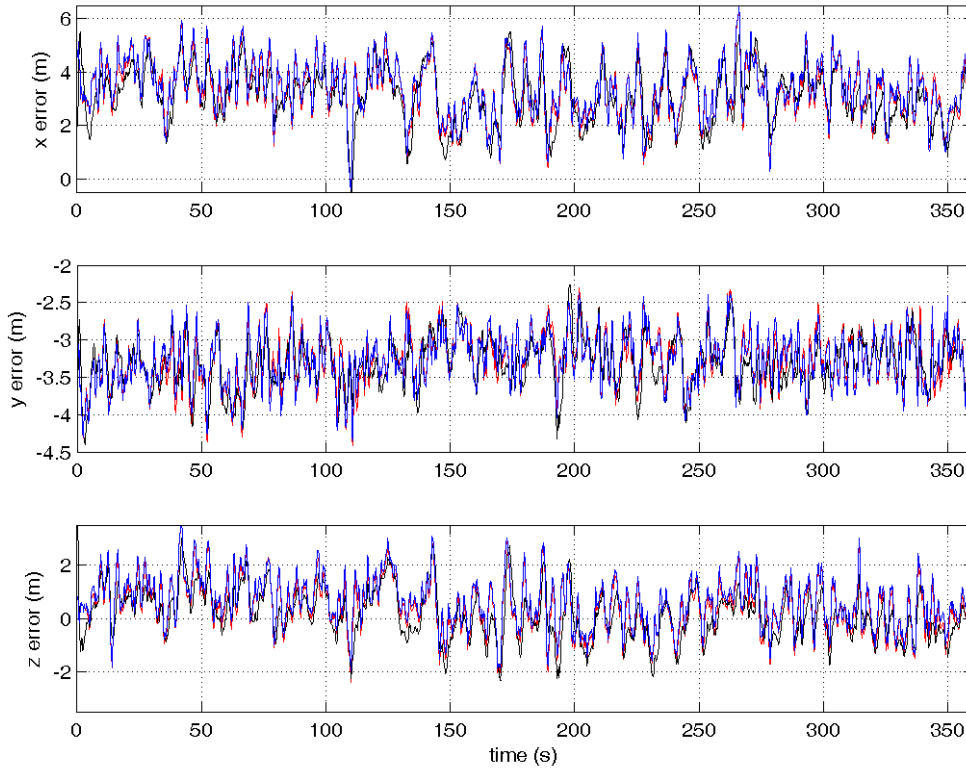


Fig. 3. Position estimation errors of nonlinear observer (red), nonlinear observer with ARE (black) and MEKF (blue). The RTK solution is used as reference.

Table 1. Comparison of estimation accuracy, averaged over whole flight trajectory.

	RMSE (x,y,z)			STD (x,y,z)		
	NLO.	3.379	3.685	3.001	2.415	0.944
NLO-ARE	3.046	3.737	3.053	2.256	0.971	2.727
MEKF	3.475	3.715	2.983	2.461	0.959	2.858

Table 2. Numerical comparison of computational complexity. The values are average number of arithmetic operations per second.

	MEKF		NLO		NLO-ARE	
	Mult.	Add.	Mult.	Add.	Mult.	Add.
Attitude observer prediction (410 Hz)	82000	102500	8200	4920	8200	4920
Attitude observer correction (410 Hz)	81180	77080	54940	41000	54940	41000
Attitude observer gain computation (410 Hz)	147600	137760	—	—	—	—
TMO prediction (5 Hz)	10845	10280	10845	10280	10845	10280
TMO correction (5 Hz)	7750	7275	7750	7275	7750	7275
TMO gain computation (5 Hz)	4250	4875	4250	4875	—	—
TMO gain computation (0.003 Hz)	—	—	—	—	3	3
Total	333625	339770	85985	73270	81738	63478

in Section 4.1 strongly indicates that no significant loss of estimation accuracy results from updating the Riccati equation at $0.003Hz$ versus $5Hz$.

5 Conclusions

Position estimation based on pseudo-range and range-rate measurements is an inherently nonlinear problem. In order to design an estimator for fusing the pseudo-range and range-rate measurements with inertial and compass measurements, we have designed a nonlinear observer where the only linearization is made with respect to the pseudo-range and

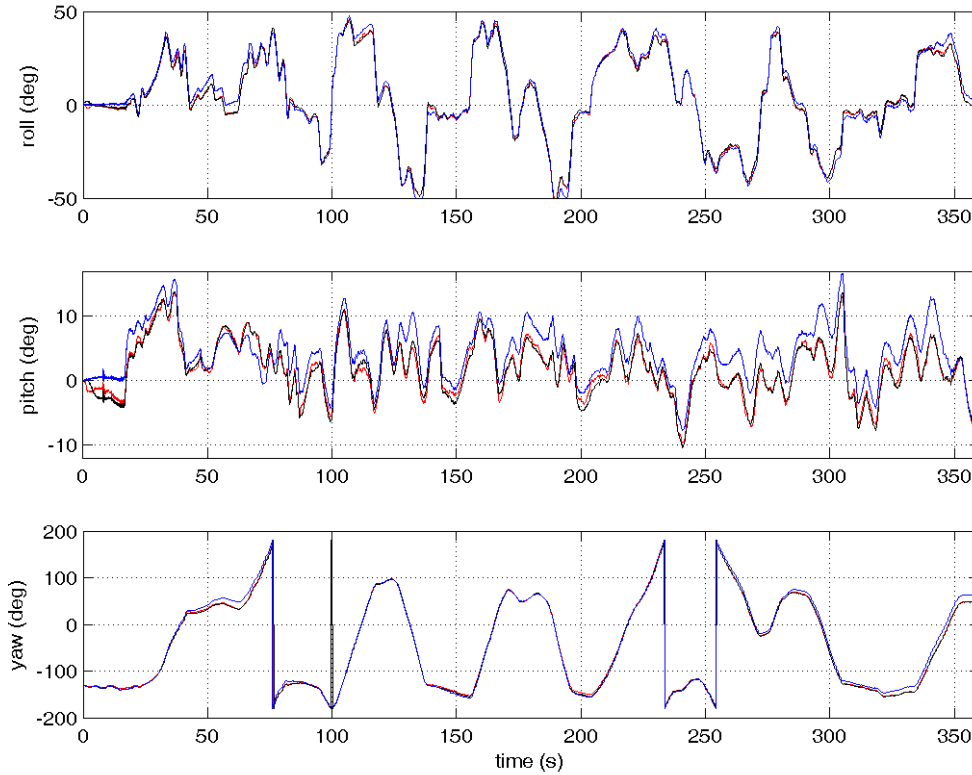


Fig. 4. Estimated attitude of nonlinear observer (red), nonlinear observer with ARE (black) and MEKF (blue).

range-rate measurement equations. The resulting observer is semiglobally exponentially stable with respect to attitude and gyro bias initialization errors, and locally exponentially stable with respect to position, velocity and acceleration initialization errors. The practical validity of the linearization is strongly motivated by the fact that a computationally simple analytic formula can be used to explicitly solve the pseudo-range equations in order to accurately initialize (or reset, if necessary) the nonlinear observer position and velocity estimates. Experimental results show that the accuracy can be comparable to an MEKF.

A key feature of the method is a time-scale separation that allows different observer blocks to be updated at different rates:

1. Instantaneous resetting of position and velocity estimates using an algebraic solution to the pseudo-range equations during initialization or change of transponder configuration. This approach justifies that only a local region of attraction may be required for the position and velocity estimates due to the good initialization accuracy.
2. Attitude estimation using a Riccati-free fixed-gain nonlinear observer, including gyro bias, on a fast time-scale driven by the sampling rate of the IMU and magnetometer.
3. Estimation of position, velocity, acceleration and error parameters for the pseudo-range measurement sys-

tem, using a nonlinear translational model observer with time-varying gains operating on a slower time-scale driven by the sampling rate of the range and range-rate sensors.

4. Computation of slowly time-varying gain matrices for the translational motion observer using a Riccati equation. These computations are made on the slowest time-scale driven by the change in relative position between the vehicle and the transponders, and for many applications it may be implemented by solving an algebraic Riccati equation periodically at low rate.

The time-scale separation can be directly exploited for computational efficiency in a multi-rate discrete-time implementation.

Acknowledgements

We thank Torleiv Bryne and Nadia Sokolova for their contributions to this paper. This work was supported by the Research Council of Norway, Statoil, DNV GL and Sintef through the Centers of Excellence funding scheme, Grant 223254 - Centre for Autonomous Marine Operations and Systems (AMOS) and the Research Council of Norway through grant 221666.

References

- [1] Farrell, J. A., 2008. *Aided Navigation. GPS with high rate sensors*. McGraw-Hill.
- [2] Grewal, M., Weill, L. R., and Andrews, A. P., 2007. *Global positioning systems, inertial navigation and integration*. Wiley.
- [3] Groves, P. D., 2013. *Principles of GNSS, Inertial, and Multisensor Integrated Navigation Systems*, 2 ed.
- [4] Gustafsson, F., 2012. *Statistical Sensor Fusion*. Studentlitteratur.
- [5] Markley, F., 2003. “Attitude error representation for kalman filtering”. *J. Guidance, Control and Dynamics*, **26**, pp. 311–317.
- [6] Crassidis, J. L., Markley, F. L., and Cheng, Y., 2007. “Survey of nonlinear attitude estimation methods”. *J. Guidance, Control and Dynamics*, **30**, pp. 12–28.
- [7] Reif, K., Sonnemann, F., and Unbehauen, R., 1998. “An EKF-based nonlinear observer with a prescribed degree of stability”. *Automatica*, **34**, pp. 1119–1123.
- [8] Grip, H. F., Fossen, T. I., Johansen, T. A., and Saberi, A., 2013. “Nonlinear observer for GNSS-aided inertial navigation with quaternion-based attitude estimation”. In Proc. American Control Conference, Washington DC.
- [9] Morgado, M., Batista, P., Oliveira, P., and Silvestre, C., 2011. “Position and velocity USBL/IMU sensor-based navigation filter”. In Proc. IFAC World Congress, Milano, pp. 13642–13647.
- [10] Batista, P., Silvestre, C., and Oliveira, P., 2013. “GAS tightly coupled LBL/USBL position and velocity filter for underwater vehicles”. In Proc. European Control Conference, Zurich, Switzerland, pp. 2982–2987.
- [11] Batista, P., 2015. “GES long baseline navigation with unknown sound velocity and discrete-time range measurements”. *IEEE Trans. Control Systems Technology*, **23**, pp. 219–230.
- [12] Batista, P., Silvestre, C., and Oliveira, P., 2014. “Sensor-based long baseline navigation: observability analysis and filter design”. *Asian J. Control*, **16**, pp. 974–994.
- [13] Batista, P., Silvestre, C., and Oliveira, P., 2015. “Tightly coupled long baseline/ultra-short baseline integrated navigation systems”. *Int. J. Systems Science*. to appear.
- [14] Batista, P., 2014. “GES long baseline navigation with clock offset estimation”. In Proc. European Control Conference, Strasbourg, France, pp. 3011–3016.
- [15] Mahoney, R., Hamel, T., and Pfimlin, J.-M., 2008. “Nonlinear complementary filters on the special orthogonal group”. *IEEE Trans. Automatic Control*, **53**, pp. 1203–1218.
- [16] Grip, H. F., Fossen, T. I., Johansen, T. A., and Saberi, A., 2012. “Attitude estimation using biased gyro and vector measurements with time-varying reference vectors”. *IEEE Trans. Automatic Control*, **57**, pp. 1332–1338.
- [17] Johansen, T. A., and Fossen, T. I., 2015. “Nonlinear observer for inertial navigation aided by pseudo-range and range-rate measurements”. In Proc. European Control Conference, Linz.
- [18] Dardari, D., Falletti, E., and Luise, M., 2012. *Satellite and Terrestrial Radio Positioning Techniques*. Academic Press.
- [19] Bancroft, S., 1985. “An algebraic solution to the GPS equations”. *IEEE Trans. Aerospace Electronic Systems*, **21**, pp. 56–59.
- [20] Chaffee, J., and Abel, J., 1994. “On the exact solutions of pseudorange equations”. *IEEE Trans. Aerospace and Electronic Systems*, **30**, pp. 1021–1030.
- [21] Yan, J., Tiberius, C. C. J. M., Janssen, G. J. M., Tennesen, P. J. G., and Bellusci, G., 2013. “Review of range-based positioning algorithms”. *IEEE Aerospace and Electronic Systems Magazine*, August, Part II, pp. 2–27.
- [22] Shuster, M., and Oh, S., 1981. “Three-axis attitude determination for vector observations”. *J. Guidance, Control and Dynamics*, **4**, pp. 70–77.
- [23] Anderson, B. D. O., 1971. “Stability properties of Kalman-Bucy filters”. *J. Franklin Institute*, **291**, pp. 137–144.
- [24] Kalman, R. E., and Bucy, R. S., 1961. “New results in linear filtering and prediction theory”. *Trans. ASME, Ser. D, J. Basic Eng*, pp. 95–109.
- [25] Khalil, H. K., 2002. *Nonlinear systems*. Prentice-Hall.
- [26] Horn, R. A., and Johnson, C. R., 2013. *Matrix Analysis*, 2 ed. Cambridge.

Appendix A - Proofs

Proof Lemma 3. It follows by Taylor’s theorem that

$$e_{y,i} = \left(\frac{\hat{p}^e - p_i^e}{\hat{\rho}_i} \right)^T \tilde{p} + \zeta_i^T \tilde{\beta} + \frac{1}{2} \tilde{p}^T \check{H}_i \tilde{p} \quad (34)$$

where

$$\check{H}_i = \frac{1}{\check{\rho}_i} I_3 - \frac{(\check{p}^e - p_i^e)(\check{p}^e - p_i^e)^T}{\check{\rho}_i^3} \quad (35)$$

where \check{p}^e is on the line between \hat{p}^e and p_i^e , $\check{\rho}_i := \|\check{p}^e - p_i^e\|_2$. The bound on $e_{y,i}$ follows using the triangle and Cauchy-Schwarz inequalities.

Applying Taylor’s theorem also gives

$$e_{v,i} = \frac{(\hat{p}^e - p_i^e)^T}{\hat{\rho}_i} \tilde{v} + \frac{(\hat{v}^e - v_i^e)^T}{\hat{\rho}_i} \tilde{p} + \varphi_i^T \tilde{\beta} + \frac{1}{2} (\tilde{p}; \tilde{v})^T \begin{pmatrix} \check{J}_i & \check{H}_i \\ \check{H}_i & 0 \end{pmatrix} (\tilde{p}; \tilde{v}) \quad (36)$$

where \check{H}_i is defined similar to (35), and it is straightforward

to show that

$$\begin{aligned} \check{J}_i &= \frac{1}{\check{\rho}_i^3} \left((\check{p}^e - p_i^e)(\check{v}^e - v_i^e)^T + \check{p}^e - p_i^e \right)^T (\check{v}^e - v_i^e) I_3 \\ &\quad - \frac{3}{\check{\rho}_i^5} (\check{p}^e - p_i^e)(\check{p}^e - p_i^e)^T (\check{p}^e - p_i^e)(\check{v}^e - v_i^e)^T \end{aligned}$$

were $\check{\rho}_i = \|\check{p}^e - p_i^e\|_2$ for some \check{p}^e on the line between p^e and \hat{p}^e , and \check{v}^e is on the line between v^e and \hat{v}^e . The bound on $\varepsilon_{v,i}$ follows using the triangle and Cauchy-Schwarz inequalities. \square

Proof Lemma 5. In order to characterize the null-space of C , let $Z \in \mathbb{R}^{n \times (n-k)}$ have $n-k$ columns that forms an orthonormal basis for the null-space of D^T and $Y \in \mathbb{R}^{n \times k}$ have $k = \text{rank}(D^T)$ columns that forms an orthonormal basis for the range-space of D^T . It follows that $D^T Z = 0$ and $\text{rank}(D^T Y) = k$. Consider a vector $x = (x_1; x_2; x_3; x_4)$, where $x_1, x_2, x_3 \in \mathbb{R}^3$ and $x_4 \in \mathbb{R}^n$. Let $x_4 = Zx_{4Z} + Yx_{4Y}$ where $x_{4Z} \in \mathbb{R}^{n-k}$ and $x_{4Y} \in \mathbb{R}^k$. The vector x belongs to the null-space of C if $Cx = 0$, which is equivalent to $M \cdot (x_1; x_2; x_4Y) = 0$ where

$$M = \begin{pmatrix} G^T & 0 & D_p^T Y \\ B^T & G^T & D_v^T Y \end{pmatrix}$$

From Assumption 6 it follows immediately that $M \in \mathbb{R}^{2m \times (6+k)}$ has rank $6+k$ and $2m \geq 6+k$. From $M \cdot (x_1; x_2; x_4Y) = 0$ it follows that the null-space of C is characterized by $x_1 = 0, x_2 = 0, x_4Y = 0$ while x_3 and x_4Z can be arbitrary.

Now, consider a singular value decomposition $C = USV^T$, where the Moore-Penrose pseudo-inverse is given by $C^+ = VS^+U^T$, cf. [26]. From the characterization of the null-space of C , we have

$$C^+C = VS^+SV^T = \text{blockdiag}(I_3, I_3, 0_3, J)$$

for some matrix $J \in \mathbb{R}^{n \times n}$, and we get $L_\theta C^+C = C^+CL_\theta$ due to both C^+C and L_θ sharing the same block diagonal structure. The result follows from $E_\theta C = CL_\theta C^+C = CC^+CL_\theta = CL_\theta$ since the Moore-Penrose pseudo-inverse satisfies $CC^+C = C$, [26]. \square

Appendix B - Observability analysis

In this appendix we study the observability Gramian $\mathcal{W}(t, t + \tau)$, where we have assumed without loss of generality that $R = I$. The state transition matrix $\Phi(T) = e^{AT}$ is straightforward to compute

$$\Phi(T) = \begin{pmatrix} I_3 & TI_3 & (T^2/2)I_3 & 0 \\ 0 & I_3 & TI_3 & 0 \\ 0 & 0 & I_3 & 0 \\ 0 & 0 & 0 & I_n \end{pmatrix}$$

We get the following expression

$$C(T)\Phi(T) = \begin{pmatrix} G^T & TG^T & \frac{T}{2}G^T & D_p^T \\ B^T & TB^T + G^T & \frac{T^2}{2}B^T + TG^T & D_v^T \end{pmatrix}$$

Let $N(T) := \Phi(T)^T C^T(T)C(T)\Phi(T) \in \mathbb{R}^{(9+n) \times (9+n)}$ be the integrand of the observability Gramian. It is instructive to consider some special cases.

Special case: Only range measurements, no pseudo-range error parameters β .

Consider the case when $n = 0$ and there are only range measurements (i.e. no range-rate measurements). Then

$$C(T)\Phi(T) = G^T \left(I_3 \quad TI_3 \quad \frac{T^2}{2}I_3 \right)$$

We get $N(T) = \Xi(T) \otimes GG^T$, where \otimes denotes the Kronecker product, and

$$\Xi(T) = \begin{pmatrix} 1 & T & \frac{T^2}{2} \\ T & T^2 & \frac{T^3}{2} \\ \frac{T^2}{2} & \frac{T^3}{2} & \frac{T^4}{4} \end{pmatrix}$$

We have $\mathcal{W}(t + \tau, t) = \int_t^{t+\tau} \Xi(T) dT \otimes GG^T$. We observe that while $\Xi(T) \in \mathbb{R}^{3 \times 3}$ has rank one, it is straightforward to prove that $\text{rank}(\int_t^{t+\tau} \Xi(T) dT) = 3$ for all $\tau > 0$. Consequently, with three linearly independent transponder positions forming G , we have that $\text{rank}(GG^T) = 3$ and $\text{rank}(\mathcal{W}(t + \tau, t)) = 9$ since $\text{rank}(A \otimes B) = \text{rank}(A) \cdot \text{rank}(B)$.

Special case: Only range measurements, with receiver clock bias.

In this case $n = 1$, and $D_p = (1, 1, 1)$ since the receiver clock bias is the same for all measurements made by the single receiver. In this case $\mathcal{W}(t + \tau, t) \in \mathbb{R}^{10 \times 10}$. Compared to the previous case, it is straightforward to see that a fourth transponder is needed such that $GG^T \in \mathbb{R}^{4 \times 4}$ has full rank in this case.